Optimal automatic detection of muscle activation intervals

Usman Rashid[a,*], Imran Khan Niazi[a,b,c], Nada Signal[a], Dario Farina[d], Denise Taylor[a]

[a] Health & Rehabilitation Research Institute, Auckland University of Technology, Auckland, New Zealand
[b] Centre for Chiropractic Research, New Zealand College of Chiropractic, Auckland, New Zealand
[c] SMI, Department of Health Science and Technology, Aalborg University, Denmark
[d] Department of Bioengineering, Imperial College London, UK

ARTICLE INFO

ABSTRACT

A significant challenge in surface electromyography (sEMG) is the accurate identification of onsets and offsets of muscle activations. Manual labelling and automatic detection are currently used with varying degrees of reliability, accuracy and time efficiency. Automatic methods still require significant manual input to set the optimal parameters for the detection algorithm. These parameters usually need to be adjusted for each individual, muscle and movement task. We propose a method to automatically identify optimal detection parameters in a minimally supervised way. The proposed method solves an optimisation problem that only requires as input the number of activation bursts in the sEMG in a given time interval. This approach was tested on an extended version of the widely adopted double thresholding algorithm, although the optimisation could be applied to any detection algorithm. sEMG data from 22 healthy participants performing a single (ankle dorsiflexion) and a multi-joint (step on/off) task were used for evaluation. Detection rate, concordance, F_1 score as an average of sensitivity and precision, degree of over detection, and degree of under detection were used as performance metrices. The proposed method improved the performance of the double thresholding algorithm in multi-joint movement and had the same performance in single joint movement with respect to the performance of the double thresholding algorithm with task specific global parameters. Moreover, the proposed method was robust when an error of up to ± 10% was introduced in the number of activation bursts in the optimisation phase regardless of the movement. In conclusion, our optimised method has improved the automation of a sEMG detection algorithm which may reduce the time burden associated with current sEMG processing.

1. Introduction

Surface electromyography (sEMG) is widely used for measurement of muscle activity in biomechanics, biomedical and sports science areas (Hogrel, 2005; Reaz et al., 2006; Massó et al., 2010; Niazi et al., 2011; Ahmadian et al., 2013; Karimi et al., 2017; Chowdhury et al., 2013; Luca, 1997; Hermens et al., 2000). From sEMG recordings, the accurate identification of intervals of muscle activity has applications in the study of different pathologies such as neck or back pain (Falla et al., 2004; Larivière et al., 2010), in analysis of event-related brain signals (Boxtel et al., 1993) and in movement rehabilitation (Kawakami et al., 2016; Cauraugh et al., 2000; Hara et al., 2013) among others. The identification of these intervals is a multifaceted challenge, due to difficulty in defining *onsets* and *offsets* (Magda, 2015), and large variability in the amplitude of the sEMG signal across different muscles, movement tasks and populations (Robichaud et al., 2009; Yang et al.,

2017). Furthermore, different applications involving online or offline processing impose different constraints of time and computational complexity (Drapała et al., 2012).

When the sEMG is processed offline, onsets and offsets are identified either automatically using an algorithm (Chowdhury et al., 2013; Yang et al., 2017; Guerrero and Macías-Díaz, 2014; Staude et al., 2001; Merlo et al., 2003), or manually labelled by an expert (Falla et al., 2004; Worsley et al., 2013; Moseley et al., 2003; Vasseljen et al., 2006; Hodges et al., 2003). The limitations of the manual labelling method are the time needed to label individual onsets/offsets and the risk of subjective bias. Whereas, automatic methods use algorithms which dictate the amplitude and duration of activity that should be classified as *on* or *off*. Nonetheless, the expert has to select an appropriate algorithm and a set of parameters for the algorithm, such as the number of standard deviations above baseline mean for sEMG activity to be classified as *on*. Fully automatic processing can be achieved by selecting a

---

* Corresponding author.
E-mail addresses: urashid@aut.ac.nz (U. Rashid), imran.niazi@aut.ac.nz (I.K. Niazi), nada.signal@aut.ac.nz (N. Signal), d.farina@imperial.ac.uk (D. Farina), denise.taylor@aut.ac.nz (D. Taylor).

single set of parameters and applying it to the entire dataset. Such a single set of parameters is referred to as *global* parameters in this paper. The automatic method involving an algorithm along with a global set of parameters is time efficient but also prone to error (Jubany and Angulo-Barroso, 2016) and has poor repeatability (Hodges and Bui, 1996). Commonly researchers use a hybrid approach with an algorithm used initially, followed by visual inspection and manual adjustment of the detected sEMG bursts. However, this still requires the expert to manually adjust the parameters of the algorithm in response to varying signal characteristics, so that the algorithm detects muscle activity appropriately. To reduce this time burden, a method is needed to optimise the detection algorithm parameters with minimal additional input from the expert.

The aim of this research is to provide a simple and efficient method to optimise sEMG detection algorithms. We achieve this by exploiting the assumption that an expert can accurately visually identify the *number of bursts* in a sEMG signal. It is more difficult to visually identify the precise onsets and offsets since this requires inspecting the signals in detail. We propose an optimisation method which takes the estimated number of sEMG bursts in the signal as the only input from the expert and finds an optimal set of parameters for the sEMG detection algorithm. The proposed method can be used in two possible ways: (i) for finding an optimal set of parameters from a single trial that has a known number of bursts and then applying these obtained optimal parameters to subsequent trials, or (ii) for finding an optimal set of parameters for each trial separately. The advantage of the first technique is that the expert has to estimate the number of sEMG bursts only in one trial. The disadvantage is that the detection algorithm may not achieve desired performance on the subsequent trials with parameters obtained from a single trial. The second technique overcomes this problem as an optimal set of parameters is obtained for each trial separately. When these optimal parameters are used to detect sEMG bursts from the same trial, it results in an optimal detection of onsets and offsets for that trial. The application of this technique may not be feasible with existing optimisation methods for which the expert has to manually select a number of different parameters some of which can be nonintuitive. With our proposed method the application of the second technique is feasible as the expert's initial input is reduced to estimating the number of bursts in the signal.

In theory the proposed optimisation method can be used with any detection algorithm which is deemed appropriate for a particular study. Here we use it in combination with an extended version of the widely adopted double thresholding algorithm (Bonato et al., 1998; Staude et al., 2001; Jubany and Angulo-Barroso, 2016). To evaluate our proposed method, we test it on sEMG data from two different lower limb tasks in a healthy population. We compare the quality of the activation bursts detected by the extended double thresholding algorithm optimised with the proposed method in each trial separately against the bursts manually labelled by an expert in that trial and the bursts detected by the extended double thresholding algorithm with task specific global parameters.

2. Methods

2.1. Proposed optimisation method

Given the number of muscle activations, an optimal set of parameters (P) was found by solving the following optimisation problem.

$$\min_{P} \quad ||n(\Lambda(P_i, X)) - N_e||_2 + \frac{N_A}{N} + \frac{E_B}{E}$$
$$B^l \leqslant P \leqslant B^u \tag{1}$$

where $n(.)$ denoted the operation which gave the number of onset/offset pairs in the set returned by the detection algorithm (Λ). The algorithm took an initial set of parameters (P_i) and a sEMG signal (X). N_e was the estimated number of onset/offset pairs supplied by the expert

as input. N_A and N denoted the number of samples contained by the detected onsets/offsets and total number of samples in the sEMG signal. E_B and E represented the energy outside the detected onsets/offsets and total energy of the sEMG signal. The Teager-Kaiser operator was used to find the energy from the sEMG signal (Solnik et al., 2010). B^l and B^u denoted the lower and the upper bounds on the parameters of the detection algorithm (Λ).

The proposed optimisation problem in Eq. (1) is a heuristic optimisation problem (Gilli, 2004; Pearl, 1984). The heuristic based on the difference between the number of estimated bursts and the number of detected bursts directed the search strategy to the nearest minimum from the initial conditions in the solution space while disregarding the quality of the detected bursts. A very fast convergence (approximately ⩽5 iterations) could be achieved by only using this heuristic, for achieving optimal quality for the detected bursts, the two balancing terms which minimise samples and maximise energy of the bursts were also used.

Solving the optimisation problem stated in Eq. (1) with a traditional derivative based search strategy, such as gradient decent (Ruder, 2016), required mathematical derivation of the gradients. Such a derivation can only be performed if the detection algorithm (Λ) is known and its processing steps are differentiable. Furthermore, the convexity of the optimisation problem in Eq. (1) has to be mathematically established for a given detection algorithm (Λ) so that a gradient based method can be used effectively. If the chosen detection algorithm (Λ) makes the optimisation problem non-convex, the quality of its solution depends heavily on the chosen initial parameters (P_i). To avoid these problems, we used the particle swarm algorithm described in Eberhart and Kennedy (1995) as the search strategy. A detailed tutorial explaining the particle swarm algorithm along with practical examples can be found in Marini and Walczak (2015). The particle swarm algorithm is a global approach to optimisation, and it can find a global or a near-global solution even when the optimisation problem is non-convex (Selvakumar and Thanushkodi, 2007; Parsopoulos and Vrahatis, 2002; Zhang et al., 2015; Rashid et al., 2019). Moreover, the particle swarm algorithm is a derivative-free method (Rios and Sahinidis, 2012), and the initial parameters (P_i) can be chosen randomly within the bounds (B^l and B^u). The optimisation problem proposed in Eq. (1) is referred to as *nOptim* method in the subsequent sections.

2.2. Extended Double Thresholding Algorithm (eDTA)

The input to the algorithm was preprocessed sEMG data and a set of parameters. A low pass and a high pass filter were used to preprocess the data. Both the filters were zero-phase to avoid adding any time delay in the signal. Additional characteristics of the filters are discussed in Section 2.3 after introducing the experimental dataset. The output was a set of pairs of onsets and offsets. The parameters of the algorithms are listed below followed by the operations briefly explained in sequence. The last three operations (5, 6, 7) can be disabled when not required by appropriately setting the corresponding parameters.

L_b: Length of the baseline segment.
K_b^{th}: The rank of the moving average value which was used to select the baseline segment.
N_{sd}: Number of standard deviations of the baseline segment.
T_{on}: Time in seconds for detecting an onset.
T_{off}: Time in seconds for detecting an offset.
T_s: Time in seconds for the shortest sEMG burst.
N_{nt}: Number of standard deviations of the root mean square (RMS) values of the detected bursts.
T_j: Time in seconds for the window in which two or more sEMG burst were joined into a single burst.

1. Baseline detection. Given a preprocessed sEMG signal, the first step was the automatic selection of a baseline segment and estimation of

baseline mean and standard deviation. This was achieved by first applying full wave rectification to the sEMG signal. This rectified signal was then passed through a moving average filter with a window length of L_b seconds. Using this moving average of the rectified signal, a baseline segment of length L_b seconds was selected from the rectified sEMG signal such that the rank of the corresponding moving average was K_b^{th}. The reason to select the K_b^{th} minimum value instead of the global minimum was that in some cases the rectified sEMG signal had a high noise content and choosing the quietest region as baseline was not the most suitable option. The baseline mean and standard deviation were estimated from the baseline segment of the rectified signal using sample mean and standard deviation formulae. It should be noted that the moving average filter was only used to select the baseline segment and the baseline mean and the standard deviation were computed from the preprocessed rectified signal without applying a moving average. Moreover, no moving average was applied to the signal in the subsequent operations of the algorithm.

2. First threshold using baseline parameters. Thresholding with baseline mean plus a number of baseline standard deviations (N_{sd}) was applied to the rectified sEMG signal to detect bursts of muscle activity. This operation resulted in a train of 1's and 0's. A run of consecutive 1's corresponded to muscle activity and a run of consecutive 0's corresponded to a muscle resting state. This operation resulted in a large number of false positives. Most of these false positives were removed by applying a second threshold (Bonato et al., 1998).

3. Second threshold using on time. In the train of 1's and 0's from the previous step, the first 1 in a run was considered the onset of muscle activity only if the run lasted for T_{on} seconds. And the last 1 in the run was considered the offset. This operation successfully removed very short runs, for example, burst trains of 1 or 2 consecutive ones. However, it also resulted in multiple onsets for a single movement.

4. Third threshold using off time. To overcome the problem of multiple onsets, another threshold was applied along the time dimension. An offset from the last operation was only considered a true offset if it was not followed by another onset for at least T_{off} seconds.

5. Prune short events. False positives resulting from short bursts in the sEMG signal were removed by applying another time threshold to all the onset/offset pairs (Merlo et al., 2003). An example of such a burst is shown in Fig. 1. Thus, an onset/offset pair which had a time difference shorter than T_s seconds was removed.

This pruning operation was applied after onsets and offsets had been defined by the on time and the off time. This operation allowed the algorithm to have a sensitive threshold for the on time (T_{on}). If a larger on time threshold was used to remove the short bursts of activity, such as the one shown in Fig. 1, it resulted in delayed onset detection. This operation decoupled the sensitivity of the algorithm in detecting onsets and its ability to remove short bursts without decreasing the sensitivity. It gave the algorithm another degree of freedom.

6. Prune non-typical bursts. In contrast to short bursts, there were situations when the sEMG signal had artefacts which last for a long time but had smaller amplitude compared to the typical bursts. An example non-typical burst is shown in Fig. 1. These bursts were removed by applying a threshold on the root mean square (RMS) value. This can be done in two ways. Either by directly specifying a RMS threshold value, or, in the case of repeated movements, by specifying the number of standard deviations (N_{nt}) to create acceptable bounds around the mean RMS value of all the detected bursts. The latter approach was adopted in this study.

7. Join movement components. Finally, this operation was introduced for situations where a movement had two components and it was desirable to represent the whole movement with one pair of an onset and an offset. For example, in the case of a step on/off a step-stool, the movement had two components. The onset/offset pairs from the two components were joined together by specifying a time window of T_j seconds.

2.3. Experimental dataset

The sEMG data used in this study was collected as part of a previously published study. Further details about the study and the experimental protocol can be found in Rashid et al. (2018).

Participants. Twenty-two healthy participants (Average age: 36 ± SD 6 years, 10 Female) took part in the experiment conducted at Auckland University of Technology, New Zealand. Participants were excluded if they had a history of any neurological disorders or epilepsy. All the participants signed a written consent form before data collection. The ethics for the study was approved by Central Health and Disability Ethics Committee (HDEC) (17/CEN/133), New Zealand in accordance with the Declaration of Helsinki.

Experimental protocol. For each participant, data was collected in one session. The participants executed 50 single joint movements (right foot ballistic ankle dorsiflexions) while seated and 50 repetitions of multi-joint movements (right foot step on and off a step-stool which was approximately 23 cm high and placed at a comfortable distance) while standing. For ankle dorsiflexion, participants were seated in an ergonomic dentist-like chair with their back slightly reclined. Their legs were supported in approximately 25 degrees knee flexion and they had their ankle in a relaxed position. They were advised to look forward, flex their right ankle by pulling their toes towards their face in fast but controlled manner. For step on/off, participants were advised to place their right foot on the step-stool and immediately bring it back to the ground. They executed the tasks at their own pace while pausing for at least five seconds between each repetition. The order of the tasks was chosen at random.

Two surface electrodes (Ambu® BlueSensor N) were placed on the right tibialis anterior (TA) muscle. The electrodes were connected to a NuAmps (Compumedics Neuroscan) amplifier which was used for impedance measurement and data recording. Preparation included shaving, exfoliating with the Nuprep Gel (Weaver and Company, USA), subsequent cleansing with disposable alcohol swabs and accepting the electrode impedance below 10 kΩ. Data was recorded with the Acquire software (Compumedics Neuroscan). The sample-rate was set at 500 Hz. Examples of sEMG bursts for ankle dorsiflexion and step on/off are shown in Fig. 2.

Signal processing. The data was processed on MATLAB 2017b (MathWorks, Inc.). The data from one sEMG electrode was subtracted from the other to form a single differential derivation. This channel was then filtered using a high pass and a low pass 2nd order, zero-phase, Butterworth filter with cut-off at 10 Hz and 200 Hz respectively.

Manual labelling by an expert. To conduct a comparison between the proposed nOptim method applied on eDTA and manual labelling, full wave rectified experimental data was manually labelled by an expert. The expert scrolled through the full wave rectified data using a custom graphical user interface (GUI) tool and manually placed onsets and offsets of muscle activity. The custom graphical user interface tool was developed on MATLAB 2017b.

2.4. Software implementation

The MATLAB 2017b based graphical user interface tool developed as part of this study is shown in Fig. 3 and has been made available online.[1] This toolbox includes the extended double thresholding algorithm and the proposed *nOptim* method. This software can be used to visually estimate the number of bursts in multi-channel sEMG data and then obtain an optimal set of bursts using the *nOptim* method against that estimate. The individual onsets/offsets can be added, removed and moved. Other algorithms can easily be added to it and used with the *nOptim* method without the need to change any GUI related code. Although the toolbox allows processing of multi-channel data, each
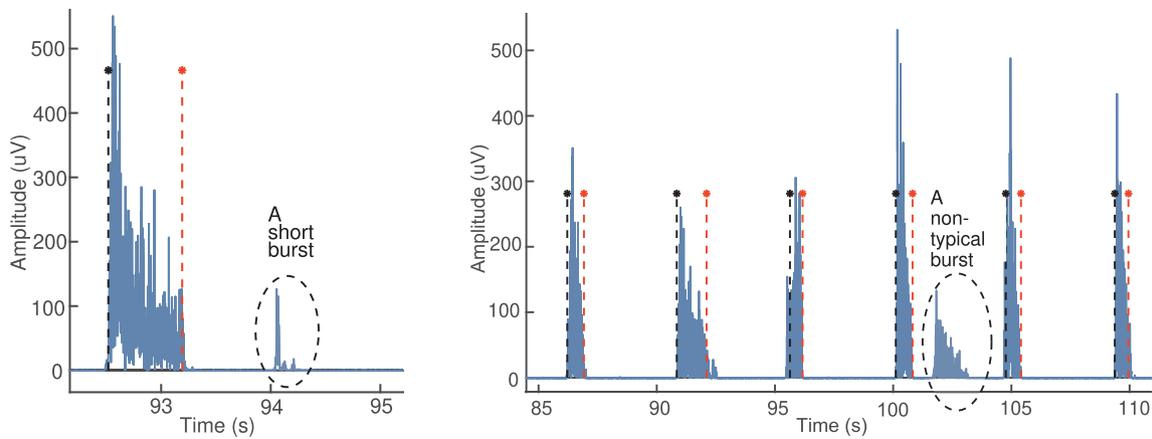
---

[1] https://github.com/GallVp/emgGO.

Fig. 1. Example of a short burst and a non-typical burst.
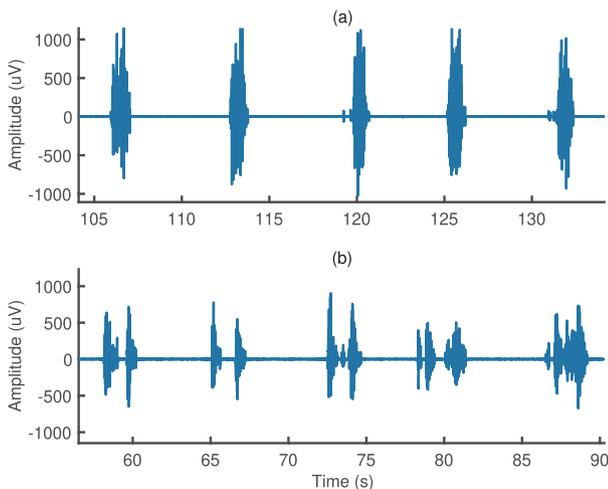
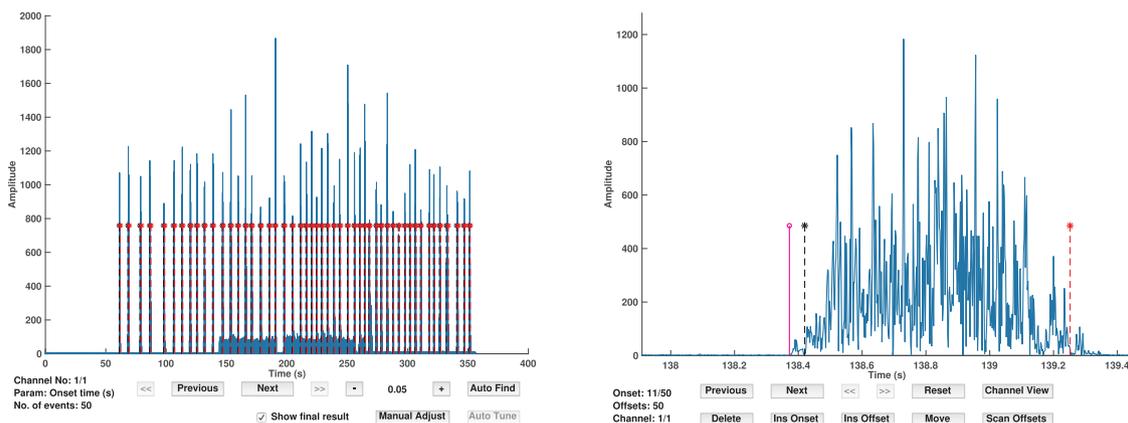**Fig. 2.** Example muscle activation bursts for ankle dorsiflexion (a) and step on/off (b).

applied on eDTA and eDTA with global parameters, a separate set of global parameters was tuned for each task. Instead of obtaining the global parameters by manual tuning, an empirical approach was taken to select the best possible parameters. For each task, data from 6 participants was chosen at random as a training set. We chose 6 participants instead of all 22 for training as it represented a practical approach where data is manually labelled for a randomly chosen smaller set and algorithm parameters are obtained from this labelled data for use with the rest of the unseen unlabelled data. An optimal set of parameters was found for each participant in the training set by minimising the following cost function.

$$\min_{P} \quad ||1 - C(\Lambda(P_i, X), R)||_2$$
$$B^l \leqslant P \leqslant B^u \qquad (2)$$

where R represented the set of onset/offset pairs manually labelled by the expert, and C denoted the concordance between the expert and the algorithm (see further details on concordance in Section 2.6.2). Particle swarm algorithm was used for optimisation. To avoid overfitting on a single participant, the obtained set of parameters was used to compute

Fig. 3. The graphical user interface (GUI) tool developed in this study. The left window shows the main GUI with options to find estimated number of onset/offset pairs. The right window shows one onset/offset pair with rectified sEMG signal. It allows the user to move, insert and delete individual events.

channel has to be processed separately as it keeps the algorithm parameters for each channel separate. This was implemented under the assumption that different channels may represent sEMG from different muscles with varied signal characteristics.

2.5. Global parameters for eDTA

To conduct a comparison between the proposed nOptim method

cross-validation cost, defined as $||1 - C(\Lambda(P, X), R)||_2$, for the remaining five participants in the training set. The set of task specific parameters which gave lowest mean leave-p-out cross-validation cost was selected and applied to all the 22 participants.

2.6. Statistical analysis

Statistical analysis was performed in MATLAB 2017b. Four

important questions needed to be answered with experimental data. First, what was the detection rate of the proposed *nOptim* method applied on eDTA and of the eDTA with global parameters, i.e., did these methods successfully produce as many onset/offset pairs as labelled by the expert? Second, what was the quality of their detections in comparison with the expert? Third, what was the quality of the detections of *nOptim* method applied on eDTA compared to the eDTA with global parameters? And fourth, what was the quality of the detections of *nOptim* method applied on eDTA if there was an error in the estimated number of onset/offset pairs as compared to the actual number of sEMG bursts present in the signal. To answer these questions we ran the *nOptim* method on eDTA for each participant and task separately. The estimated number of onset/offset pairs (N_e in Section 2.1) was set equal to the number of onset/offset pairs manually labelled by the expert. For the eDTA, results were obtained using the task specific global parameters as explained in Section 2.5. The methods used to investigate these four questions are detailed in the following subsections.

2.6.1. Detection rate

Detection rate (DR) was obtained to quantify the difference in the number of detected pairs of onsets/offsets and the number of pairs manually labelled by the expert. It was defined as the percentage of the number of onset/offset pairs detected by the algorithm to the number of sEMG bursts labelled by the expert. It was obtained for both the *nOptim* method applied on eDTA and for eDTA with the global parameters. Statistical tests were performed to evaluate differences across the methods. Statistical tests are explained later in Section 2.6.3.

2.6.2. Comparison with the expert

To answer the second question we obtained concordance (CO), degree of over detection (OD), degree of under detection (UD) and F_1 score (a combined measure of sensitivity and precision). These measures were defined in terms of following quantities and expressed as percentages (Jubany and Angulo-Barroso, 2016).

- True positives (TPs): sEMG signal samples classified as burst by both the expert and the algorithm.
- False positives (FPs): Signal samples classified as burst by the algorithm and not by the expert.
- True negatives (TNs): Signal samples not classified as burst by both the algorithm and the expert.
- False negatives (FNs): Signal samples not classified as burst by the algorithm and classified as burst by the expert.

CO was defined as the percentage of the sum of TPs and TNs to total number of signal samples. OD was defined as the percentage of FPs to the sum of TPs and FNs. UD was defined as the percentage of FNs to the sum of TNs and FPs. F_1 score was defined as the harmonic mean of the sensitivity and precision as follows:

$$F_1 = 2 \times \frac{sensitivity \times precision}{sensitivity + precision} \times 100 = \frac{2 \times TPs}{2 \times TPs + FNs + FPs} \times 100$$

Where sensitivity (true positive rate) and precision (positive predictive value) were defined as follows.

$$Sensitivity = \frac{TPs}{TPs + FNs} \times 100$$

$$Precision = \frac{TPs}{TPs + FPs} \times 100$$

CO was interpreted as the level of agreement between the algorithm and the expert in correctly classifying the signal as *on* or *off*. F_1 was interpreted as the combined measure of the sensitivity and the precision of the algorithm compared to the expert. OD/UD were interpreted as the degree to which the algorithm detected the onset early/late and detected the offset late/early with respect to the expert.

2.6.3. eDTA with nOptim versus eDTA with global parameters

The third question was answered by comparing CO, F_1, UD and OD obtained with the proposed *nOptim* method applied on eDTA against eDTA with global parameters. Medians, inter quartile ranges, minimum and maximum values were reported for the measures as the performance measures exhibited substantial skew and large number of outliers. We tested for the equality of medians across the two methods (*nOptim* vs. Global) within each task. For comparison of medians, Wilcoxon's signed rank test with *approximate* method was performed. Significance level was set at 0.05.

2.6.4. Sensitivity to Induced Error

The fourth question was answered by running the proposed *nOptim* method on eDTA with an error introduced in the estimated number of onset/offset pairs for all the participants. Concordance was used for evaluation of its performance under ± 0%, ± 2%, ± 4%, ± 6%, ± 8% and ± 10% error. For example, if the expert had labelled 50 onset/offset pairs for a participant, an error of ± 10% was induced by running the *nOptim* method on eDTA with the estimated number of onset/offset pairs (N_e in Section 2.1) set to either 45 or 55 chosen at random.

To test the statistical significance of the differences in concordance across different levels of induced error, we performed a Friedman's test with levels of error as the column factor and movement type as the block factor. Significance level was set at 0.05. One important limitation of the Friedman's test is that despite being a two-way model it does not test for the interaction effect or the row effects. It only tests the column effects after adjusting for the row effects (Hogg and Ledolter, 1987; Hollander et al., 2015). However, the advantage of using the Friedman's test is that it accounts for the repeated measures in the data (Bewick et al., 2004).

3. Results

3.1. Global parameters for eDTA

The results for global parameter selection are shown in Fig. 4. For dorsiflexion, parameters from the 2nd training set were selected as they produced lowest mean cross-validation cost. The parameters were {0.152, 5, 2, 0.01, 0.968, 0.012, 4, 0} in the following order {L_b, K_b^{th}, N_{sd}, T_{on}, T_{off}, T_s, N_{nt}, T_j}. In the same order, parameters for step on/off were selected from the 3rd set, {0.28, 40, 2, 0.01, 1, 0.01, 7,
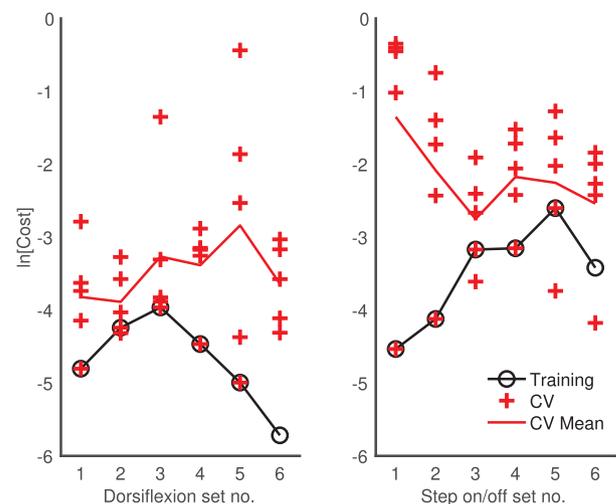

Fig. 4. Training and cross-validation natural log costs for selection of global parameters for the extended double thresholding algorithm. Cross-validation costs were computed using leave-p-out cross-validation. p was five in this case. Costs were plotted on the log scale as most of the individual cross-validation costs were too close to be distinguished from each other when plotted on a linear scale.

Table 1

Medians, inter-quartile ranges, minimum and maximum values and results of significance tests for equality of medians. Note: M_g and M_n stand for median of the measure with global parameters and median of the measure with *nOptim* parameters. H_0 stands for the null hypothesis.

Measure	Movement	Median $\pm$ IQR [min, max] %		H_0: $M_g = M_n$
		With global	With proposed *nOptim*	z-value, p-value
Detection rate	Dorsiflexion	100 $\pm$ 0 [0, 120]	100 $\pm$ 0 [100, 100]	-0.534, 0.594
	Step on/off	101.9 $\pm$ 4 [0, 142.9]	100 $\pm$ 0 [100, 100]	0.761, 0.447
Concordance	Dorsiflexion	97.7 $\pm$ 3.5 [68.7, 99.6]	96.7 $\pm$ 3.8 [87.7, 99.1]	1.055, 0.291
	Step on/off	92.2 $\pm$ 13.8 [64.9, 98.5]	94.8 $\pm$ 6.9 [79.5, 98.7]	-1.997, 0.046
F_1 score	Dorsiflexion	92.7 $\pm$ 7.9 [0, 98.1]	87.7 $\pm$ 6.5 [73.8, 96.2]	1.088, 0.277
	Step on/off	87.5 $\pm$ 15 [0, 95.5]	89.7 $\pm$ 8.7 [77.0, 97.2]	-1.997, 0.046
Degree under	Dorsiflexion	1.2 $\pm$ 1.6 [0.1, 21.3]	3.7 $\pm$ 5.7 [1, 17.9]	-2.841, 0.005
Detect	Step on/off	4.4 $\pm$ 19.5 [1.2, 56.7]	5.9 $\pm$ 9.6 [1.2, 15.1]	0.666, 0.506
Degree over	Dorsiflexion	1.3 $\pm$ 14.2 [0, 221.2]	0 $\pm$ 0 [0, 0.1]	3.621, < 0.001
Detect	Step on/off	2.4 $\pm$ 21.5 [0, 38.8]	2.1 $\pm$ 7.7 [0, 29]	0.643, 0.520

1.456}. The units of time parameters were seconds. These global parameters were used to detect onsets/offsets for all the 22 participants.

3.2. Detection rate

The detection rate for the *nOptim* method applied on eDTA was 100% for all the participants in both tasks. On the other hand the detection rate with the global parameters ranged from 0 to 120% and 0 to 143% in dorsiflexion and step on/off respectively. However, there were no statistically significant differences in the median detection rate of two methods. Detailed results are presented in Table 1. These results indicate that *nOptim* method did always converge to the estimated number of onset/offset pairs.

3.3. eDTA with nOptim versus eDTA with global parameters

Concordance, F_1 score, degree of under detection and over detection of eDTA against the expert with the *nOptim* method and the global parameters are shown in Fig. 5. Medians, inter-quartile ranges, minimum and maximum values and results of significance tests for equality of medians are presented in Table 1. These results indicated that the *nOptim* parameters generally resulted in performance metrics with smaller variability compared to the global parameters.

The differences in the median performance of the two methods were more subtle. In the case of dorsiflexion, there were no statistically significant differences in the median concordance or F_1 score across the two methods. In the case of step on/off, both the median concordance

and the median F_1 score of the *nOptim* parameters were higher compared to the global parameters. These results indicated that the *nOptim* parameters resulted in same (ankle dorsiflexion) or better (step on/off) concordance and F_1 score compared to the global parameters. Thus, the *nOptim* method did not only produce the required number of onset/offset pairs, it also produced results which were in good agreement with the expert.

In the case of dorsiflexion, the *nOptim* parameters resulted in higher degree of under detection and lower degree of over detection compared to the global parameters. In the case of step on/off, there were no statistically significant differences across the two methods in both the degree of under detection and over detection. These results indicated that the *nOptim* method resulted in same (step on/off) or higher under detection (ankle dorsiflexion) compared to the global parameters. These results are further discussed later in Section 4.

3.4. Sensitivity to induced error

The percentage concordance with zero up to $\pm10\%$ error is shown in Fig. 6. A smooth decrease in median concordance and increase in variability with an increase in error was observed. There was no statistically significant ($\chi^2 = 6.39$, p = 0.27) difference in median concordance across different levels of induced error. These results suggested that the *nOptim* method was robust to error in the estimated number of sEMG bursts.
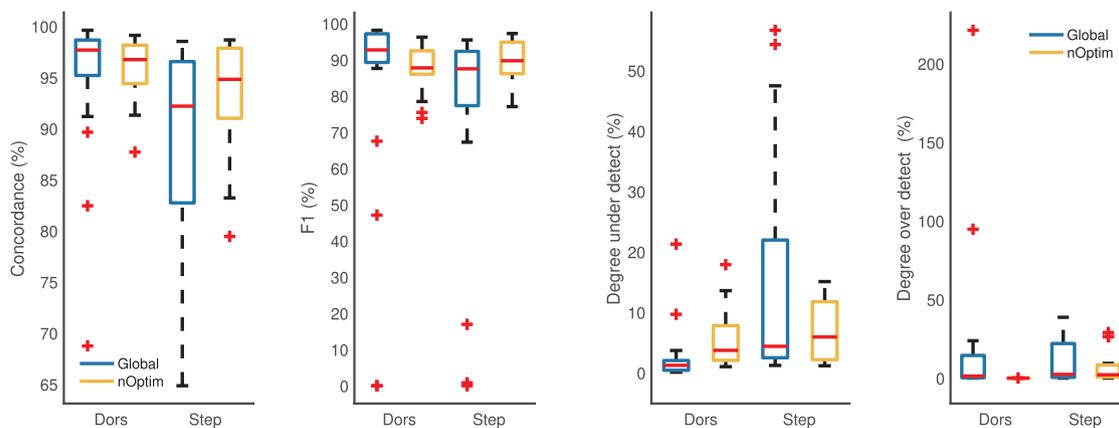

Fig. 5. Movement wise results for concordance, F_1 score, degree of over detection and under detection with global parameters and the proposed *nOptim* method. Note: Dors stands for dorsiflexion and Step for step on/off. Each box represent data from the 22 participants. The statistic line represents the median. The edges represent 1st and 3rd quartiles (Q_1 and Q_3). The lower and upper whiskers are at Q_1-1.5(Q_3-Q_1) and Q_3+1.5(Q_3-Q_1) respectively.
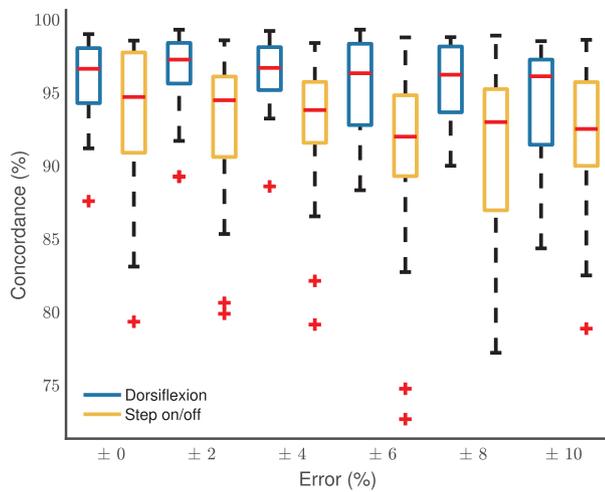
Fig. 6. Concordance between the expert and the algorithm using the proposed *nOptim* method with increasing percentage of induced error in the estimated number of sEMG activation bursts. Note: Each box represent data from the 22 participants. The statistic line represents the median. The edges represent 1st and 3rd quartiles (Q_1 and Q_3). The lower and upper whiskers are at Q_1-1.5(Q_3-Q_1) and Q_3+1.5(Q_3-Q_1) respectively.

4. Discussion

We have proposed an optimisation method (*nOptim*) for sEMG detection algorithms. We have evaluated it as a method that can be used to obtain an optimised set of sEMG bursts from a trial given an estimate of the number of bursts in the trial. Its ability to optimise burst detection based on the estimated number of bursts is the key feature which stands out from previous optimisation methods in the sEMG literature (Staude et al., 2001). On sEMG data from 22 healthy participants executing single and multi-joint movements, the proposed *nOptim* method applied on an extended version of the double thresholding algorithm has shown good agreement with the bursts manually labelled by an expert in terms of concordance, F_1 score as an average of sensitivity and precision, degree of over detection and degree of under detection. When compared against bursts detected using eDTA with global parameters, the proposed *nOptim* method had same (single joint movement) or better (multi-joint movement) performance in terms of concordance, sensitivity and precision. However, the proposed *nOptim* method had a tendency to under detect sEMG bursts in the single joint movement compared to the global parameters.

4.1. eDTA and selection of global parameters

We have also extended the double thresholding algorithm and have proposed a method for selection of global parameters. The global parameter selection method can be used to tune parameters from a smaller set of data manually labelled by an expert and apply these parameters to the rest of the unseen unlabelled data. Although the performance of eDTA with global parameters selected using this method was less consistent compared to the *nOptim* method, it may be useful to researchers interested in deploying sEMG detection algorithms on small portable low power devices which cannot afford to run an optimisation routine for each data recording (Balouchestani and Krishnan, 2014; Pashaei et al., 2015).

4.2. Detection rate

The proposed method detected 100% of the number of sEMG bursts identified by the expert across all the participants in both single joint and multi-joint movements. These results are in agreement with the results of optimisation methods previously proposed (Staude et al.,

2001). However, our proposed method only requires a single input from the user to perform the optimisation and minimal time in manually analysing the signal.

4.3. eDTA with nOptim versus eDTA with global parameters

Compared to the bursts detected by the extended double thresholding algorithm with the global parameters, the proposed *nOptim* method generally had smaller variability in concordance, F_1 score, degree of under detection and over detection. The worst case outliers for concordance and F_1 score were above 70%, and below 20% for degree of under detection and over detection. A smaller variability in performance metrices suggests better consistency with implications for the amount of time spent by the expert on adjusting the onsets and offsets detected by using an algorithm.

The *nOptim* method had same median concordance and F_1 score in the single joint movement compared to the global parameters. Whereas it had higher concordance and F_1 score in the multi-joint movement. This difference may be explained by the fact that the *nOptim* method optimised the sEMG burst detection for each participant individually while the global parameters were applied under the assumption that sEMG signal has adequate similarity across participants. As multi-joint movements involve larger number of degrees of freedom, it is reasonable to expect that different participants used different strategies in performing these movements and recruiting their muscles. Thus, *nOptim* performed better in the case of the multi-joint movement as it did not require the assumption that the sEMG signal from different participants was similar.

The degree of under detection with the proposed method was higher in the single joint movement compared to the extended double thresholding algorithm with the global parameters. This is perhaps due to the fact that the proposed method minimises the number of samples contained in the detected bursts while maximising the Teager-Kaiser energy. Although it requires further investigation, we hypothesise that the degree of under detection could be improved by adding weights to different terms in the cost function.

4.4. Sensitivity to induced error

We also investigated the sensitivity of the proposed method to induced error in the estimated number of onsets/offsets compared to the actual number of bursts present in the sEMG data. The results showed that with up to ± 10% error in the estimated number of onset/offset pairs, the worst case outlier for concordance remained above 70%. However, a gradual decrease in median concordance and increase in variability was observed. These results suggest that the proposed method has a degree of tolerance to inaccuracy in the estimate of the number of sEMG bursts and its performance does not drop strikingly.

4.5. Limitations

The findings from this research should be considered in light of a number of factors. First, the cost function used for tuning the global parameters was based on the concordance measure which was also used for comparing the *nOptim* method against the global parameters. This favoured the performance of the global parameters as they were specifically optimised to perform better in terms of the concordance measure. Thus the comparison was likely conservative and aligned against the proposed *nOptim* method. Second, although particle swarm optimisation is a global approach to optimisation, a failure to detect the required number of onsets/offsets can be expected in some situations as the proposed method is not guaranteed to result in the global optimum. In such a case, running the optimisation with different initial conditions can help convergence to a more optimal solution. Third, a single expert manually labelled the sEMG data and their results were treated as the gold standard. This was done under the assumption that the results of

manual labelling are reliable and repeatable (Jubany and Angulo-Barroso, 2016; Hodges and Bui, 1996). Fourth, the quantitative measures, such as concordance, used to evaluate the performance of the proposed methods do not measure the exact timing of the onsets and the offsets.

4.6. Recommendations for future work

The potential of the proposed *nOptim* method has not be fully evaluated yet. It may prove to be more useful with following future works.

1. A possible direction for future work is the use of the proposed *nOptim* method to obtain a global set of detection parameters that can be generalised across trials or within a long recording file. This might require adding a regularisation term to its cost function (Rakitianskaia and Engelbrecht, 2014). This approach may allow to optimise the parameters with the proposed *nOptim* method using a relatively short initial segment of the signal and then applying the optimised detection to the rest of the recording.
2. In this study we have used particle swarm optimisation as the search strategy for the proposed *nOptim* method. This allowed us to perform the optimisation without deriving the gradients of the cost function. The downside of this approach is that the particle swarm optimisation is a computationally expensive algorithm. This opens two possible directions for future work. First, to choose a detection algorithm which would allow derivation of gradients for the *nOptim* cost function and use a less computationally expensive search strategy such as gradient decent. Second, to evaluate the proposed *nOptim* method with a real-time implementation of the particle swarm algorithm (Liu et al., 2008).
3. sEMG data for both the single joint and the multi-joint movement in this study was processed as a single channel. Thus, a possible direction for future work is the evaluation of the proposed *nOptim* method on a movement, for example continuous walking, in which multi-channel data is recorded from different muscles which have different patterns of activation (Brantley et al., 2018). This, however, may also require using a detection algorithm other than the proposed extended double thresholding algorithm.

5. Conclusion

The proposed *nOptim* method can be used to obtain accurate estimates of onsets and offsets of muscle activity from a sEMG signal by simply inputting an estimate of the number of muscle activation bursts in the signal. The *nOptim* method exhibited good performance in terms of detection rate, concordance, F_1 score (sensitivity and precision), degree of under detection and over detection on sEMG data for both single joint and multi-joint movements manually labelled by an expert. This method may reduce the time burden associated with current sEMG processing.

Financial disclosure

None.

Declaration of Competing Interest

None.

Acknowledgements

References

Ahmadian, P., Cagnoni, S., Ascari, L., 2013. How capable is non-invasive eeg data of predicting the next movement? a mini review. Front. Hum. Neurosci. 7, 124. https://doi.org/10.3389/fnhum.2013.00124.
Balouchestani, M., Krishnan, S., 2014. Effective low-power wearable wireless surface emg sensor design based on analog-compressed sensing. Sensors 14 (12), 24305–24328. https://doi.org/10.3390/s141224305.
Bewick, V., Cheek, L., Ball, J., 2004. Statistics review 10: further nonparametric methods. Crit. Care 8 (3), 196. https://doi.org/10.1186/cc2857.
Bonato, P., D'Alessio, T., Knaflitz, M., 1998. A statistical method for the measurement of muscle activation intervals from surface myoelectric signal during gait. IEEE Trans. Biomed. Eng. 45 (3), 287–299. https://doi.org/10.1109/10.661154.
Boxtel, G.J.M., Geraats, L.H.D., Berg-Lenssen, M.M.C., Brunia, C.H.M., 1993. Detection of emg onset in erp research. Psychophysiology 30 (4), 405–412. https://doi.org/10.1111/j.1469-8986.1993.tb02062.x.
Brantley, J.A., Luu, T.P., Nakagome, S., Zhu, F., Contreras-Vidal, J.L., 2018. Full body mobile brain-body imaging data during unconstrained locomotion on stairs, ramps, and level ground. Scientific Data 5, 180133. https://doi.org/10.1038/sdata.2018.133.
Cauraugh, J., Light, K., Kim, S., Thigpen, M., Behrman, A., 2000. Chronic motor dysfunction after stroke. Stroke 31 (6), 1360–1364. https://doi.org/10.1161/01.str.31.6.1360.
Chowdhury, R., Reaz, M., Ali, M., Bakar, A., Chellappan, K., Chang, T., 2013. Surface electromyography signal processing and classification techniques. Sensors 13 (9), 12431–12466. https://doi.org/10.3390/s130912431.
Drapała, J., Brzostowski, K., Szpala, A., Rutkowska-Kucharska, A., 2012. Two stage emg onset detection method. Arch. Control Sci. 22 (4), 427–440. https://doi.org/10.2478/v10170-011-0033-z.
Eberhart, R., Kennedy, J., 1995. A new optimizer using particle swarm theory. In: Proceedings of the Sixth International Symposium on Micro Machine and Human, Science, IEEE. IEEE, pp. 39–43. https://doi.org/10.1109/mhs.1995.494215.
Falla, D., Jull, G., Hodges, P.W., 2004. Feedforward activity of the cervical flexor muscles during voluntary arm movements is delayed in chronic neck pain. Exper. Brain Res. 157 (1), 43–48. https://doi.org/10.1007/s00221-003-1814-9.
Gilli, M., 2004. An introduction to optimization heuristics, in: Seminar university of cyprus department of public and business administration. <http://www.unige.ch/ses/dsec/static/gilli/CyprusLecture2004.pdf>.
Guerrero, J.A., Macías-Díaz, J.E., 2014. A computational method for the detection of activation/deactivation patterns in biological signals with three levels of electric intensity. Math. Biosci. 248, 117–127. https://doi.org/10.1016/j.mbs.2013.12.010.
Hara, Y., Obayashi, S., Tsujiuchi, K., Muraoka, Y., 2013. The effects of electromyography-controlled functional electrical stimulation on upper extremity function and cortical perfusion in stroke patients. Clin. Neurophysiol. 124 (10), 2008–2015. https://doi.org/10.1016/j.clinph.2013.03.030.
Hermens, H.J., Freriks, B., Disselhorst-Klug, C., Rau, G., 2000. Development of recommendations for semg sensors and sensor placement procedures. J. Electromyogr. Kinesiol. 10 (5), 361–374. https://doi.org/10.1016/s1050-6411(00)00027-4.
Hodges, P.W., Bui, B.H., 1996. A comparison of computer-based methods for the determination of onset of muscle contraction using electromyography. Electroencephalography Clin. Neurophysiol./Electromyogr. Motor Control 101 (6), 511–519. https://doi.org/10.1016/s0921-884x(96)95190-5.
Hodges, P.W., Moseley, G.L., Gabrielsson, A., Gandevia, S.C., 2003. Experimental muscle pain changes feedforward postural responses of the trunk muscles. Exp. Brain Res. 151 (2), 262–271. https://doi.org/10.1007/s00221-003-1457-x.
Hogg, R.V., Ledolter, J., 1987. Engineering Statistics. Macmillan Pub Co.
Hogrel, J.-Y., 2005. Clinical applications of surface electromyography in neuromuscular disorders. Neurophysiologie Clinique/Clin. Neurophysiol. 35 (2–3), 59–71. https://doi.org/10.1016/j.neucli.2005.03.001.
Hollander, M., Wolfe, D.A., Chicken, E., 2015. Nonparametric Statistical Methods, vol. 751 John Wiley & Sons doi: 10.1002/9781119196037.
Jubany, J., Angulo-Barroso, R., 2016. An algorithm for detecting emg onset/offset in trunk muscles during a reaction- stabilization test. J. Back Musculoskeletal Rehabil. 29 (2), 219–230. https://doi.org/10.3233/BMR-150617.
Karimi, F., Kofman, J., Mrachacz-Kersting, N., Farina, D., Jiang, N., 2017. Detection of movement related cortical potentials from eeg using constrained ica for brain-computer interface applications. Front. Neurosci. 11, 356. https://doi.org/10.3389/fnins.2017.00356.
Kawakami, M., Fujiwara, T., Ushiba, J., Nishimoto, A., Abe, K., Honaga, K., Nishimura, A., Mizuno, K., Kodama, M., Masakado, Y., Liu, M., 2016. A new therapeutic application of brain-machine interface (bmi) training followed by hybrid assistive neuromuscular dynamic stimulation (hands) therapy for patients with severe hemiparetic stroke: a proof of concept study. Restorative Neurol. Neurosci. 34 (5), 789–797. https://doi.org/10.3233/rnn-160652.
Larivière, C., Forget, R., Vadeboncoeur, R., Bilodeau, M., Mecheri, H., 2010. The effect of sex and chronic low back pain on back muscle reflex responses. Eur. J. Appl. Physiol.

109 (4), 577–590. https://doi.org/10.1007/s00421-010-1389-7.

Liu, L., Liu, W., Cartes, D.A., Zhang, N., 2008. Real time implementation of particle swarm optimiation based model parameter identification and an application example. In: IEEE Congress on Evolutionary Computation, 2008. CEC 2008. (IEEE World Congress on Computational Intelligence). IEEE, pp. 3480–3485. doi:https://doi.org/10.1109/cec.2008.4631268.

Luca, C.J.D., 1997. The use of surface electromyography in biomechanics. J. Appl. Biomech. 13 (2), 135–163. https://doi.org/10.1123/jab.13.2.135.

Magda, M., 2015. Emg onset detection–development and comparison of algorithms, mathesis, Faculty of Computing, Blekinge Institute of Technology, SE-371 79 Karlskrona, Sweden. < https://www.diva-portal.org/smash/get/diva2:840646/FULLTEXT02.pdf >.

Marini, F., Walczak, B., 2015. Particle swarm optimization (pso). a tutorial. Chemometrics Intell. Lab. Syst. 149, 153–165. https://doi.org/10.1016/j.chemolab.2015.08.020.

Massó, N., Rey, F., Romero, D., Gual, G., Costa, L., Germán, A., 2010. Surface electromyography applications. Apunts Medicina de l Esport (English Edition) 45 (165), 121–130.

Merlo, A., Farina, D., Merletti, R., 2003. A fast and reliable technique for muscle activity detection from surface emg signals. IEEE Trans. Biomed. Eng. 50 (3), 316–323. https://doi.org/10.1109/tbme.2003.808829.

Moseley, G.L., Hodges, P.W., Gandevia, S.C., 2003. External perturbation of the trunk in standing humans differentially activates components of the medial back muscles. J. Physiol. 547 (2), 581–587. https://doi.org/10.1113/jphysiol.2002.024950.

Niazi, I.K., Jiang, N., Tiberghien, O., Nielsen, J.F., Dremstrup, K., Farina, D., 2011. Detection of movement intention from single-trial movement-related cortical potentials. J. Neural Eng. 8 (6), 066009. https://doi.org/10.1088/1741-2560/8/6/066009.

Parsopoulos, K., Vrahatis, M., 2002. Recent approaches to global optimization problems through particle swarm optimization. Nat. Comput. 1 (2–3), 235–306. https://doi.org/10.1023/a:1016568309421.

Pashaei, A., Yazdchi, M.R., Marateb, H.R., 2015. Designing a low-noise, high-resolution, and portable four channel acquisition system for recording surface electromyographic signal. J. Med. Signals Sens. 5 (4), 245–252.

Pearl, J., 1984. Heuristics: intelligent search strategies for computer problem solving.

Rakitianskaia, A., Engelbrecht, A., 2014. Weight regularisation in particle swarm optimisation neural network training. In: Weight Regularisation in Particle Swarm Optimisation Neural Network Training. IEEE, pp. 1–8. https://doi.org/10.1109/sis.2014.7011773.

Rashid, U., Niazi, I.K., Signal, N., Taylor, D., 2018. An eeg experimental study evaluating the performance of texas instruments ads1299. Sensors 18, 3721. https://doi.org/10.3390/s18113721.

Rashid, U., Niazi, I.K., Jochumsen, M., Krol, L.R., Signal, N., Taylor, D., 2019. Automated labelling of movement-related cortical potentials using segmented regression. IEEE Trans. Neural Syst. Rehabil. Eng. 1. https://doi.org/10.1109/tnsre.2019.2913880.

Reaz, M.B.I., Hussain, M.S., Mohd-Yasin, F., 2006. Techniques of emg signal analysis: detection, processing, classification and applications. Biol. Procedures online 8 (1), 11–35. https://doi.org/10.1251/bpo115.

Rios, L.M., Sahinidis, N.V., 2012. Derivative-free optimization: a review of algorithms and comparison of software implementations. J. Global Optim. 56 (3), 1247–1293. https://doi.org/10.1007/s10898-012-9951-y.

Robichaud, J.A., Pfann, K.D., Leurgans, S., Vaillancourt, D.E., Comella, C.L., Corcos, D.M., 2009. Variability of emg patterns: a potential neurophysiological marker of parkinson's disease? Clin. Neurophysiol. 120 (2), 390–397. https://doi.org/10.1016/j.clinph.2008.10.015.

Ruder, S., 2016. An overview of gradient descent optimization algorithms, arXiv e-printsarXiv:1609.04747. < https://ui.adsabs.harvard.edu/abs/2016arXiv160904747R >.

Selvakumar, A.I., Thanushkodi, K., 2007. A new particle swarm optimization solution to nonconvex economic dispatch problems. IEEE Trans. Power Syst. 22 (1), 42–51. https://doi.org/10.1109/tpwrs.2006.889132. http://adsabs.harvard.edu/abs/2007ITPSy.22...42S.

Solnik, S., Rider, P., Steinweg, K., DeVita, P., Hortobágyi, T., 2010. Teager–kaiser energy operator signal conditioning improves emg onset detection. Eur. J. Appl. Physiol. 110 (3), 489–498. https://doi.org/10.1007/s00421-010-1521-8.

Staude, G., Flachenecker, C., Daumer, M., Wolf, W., 2001. Onset detection in surface electromyographic signals: a systematic comparison of methods. EURASIP J. Appl. Signal Process. 2001 (1), 67–81. https://doi.org/10.1155/s1110865701000191.

Vasseljen, O., Dahl, H.H., Mork, P.J., Torp, H.G., 2006. Muscle activity onset in the lumbar multifidus muscle recorded simultaneously by ultrasound imaging and intramuscular electromyography. Clin. Biomech. 21 (9), 905–913. https://doi.org/10.1016/j.clinbiomech.2006.05.003.

Worsley, P., Warner, M., Mottram, S., Gadola, S., Veeger, H.E.J., Hermens, H., Morrissey, D., Little, P., Cooper, C., Carr, A., Stokes, M., 2013. Motor control retraining exercises for shoulder impingement: effects on function, muscle activation, and biomechanics in young adults. J. Shoulder Elbow Surg. 22 (4), e11–e19. https://doi.org/10.1016/j.jse.2012.06.010.

Yang, D., Zhang, H., Gu, Y., Liu, H., 2017. Accurate emg onset detection in pathological, weak and noisy myoelectric signals. Biomed. Signal Process. Control 33, 306–315. https://doi.org/10.1016/j.bspc.2016.12.014.

Zhang, Y., Wang, S., Ji, G., 2015. A comprehensive survey on particle swarm optimization algorithm and its applications. Math. Probl. Eng. 2015, 1–38. https://doi.org/10.1155/2015/931256.